Pro chondrogenic effect of mesenchymal stromal cell-based treatment of chondral defects under physioxia in a novel *ex vivo* organ model

Andrea Schwab [1], Alexa Buß [1], Oliver Pullig [1, 2], Franziska Ehlicke [1,$]

[1] University Hospital Wuerzburg, Department Tissue Engineering and Regenerative Medicine, Roentgenring 11, 97070 Wuerzburg, Germany

[2] Fraunhofer Institute for Silicate Research ISC, Translational Center Regenerative Therapies, Roentgenring 11, 97070 Wuerzburg, Germany

Andrea Schwab

- University Hospital Wuerzburg, Department Tissue Engineering and Regenerative Medicine
- Present address: AO Research Institute Davos, Clavadelerstrasse 8, 7270 Davos, Switzerland
  E-Mail: andrea.schwab@aofoundation.org

Alexa Buß

- University Hospital Wuerzburg, Department Tissue Engineering and Regenerative Medicine, Roentgenring 11, 97070 Wuerzburg, Germany
- Present address: Klinikum Würzburg Mitte gGmbH, Juliusspital, Juliuspromenade 19, 97070 Wuerzburg, Germany
  E-Mail: alexa.buss@kwm-klinikum.de

Oliver Pullig

- University Hospital Wuerzburg, Department Tissue Engineering and Regenerative Medicine, Roentgenring 11, 97070 Wuerzburg, Germany
- Fraunhofer Institute for Silicate Research ISC, Translational Center Regenerative Therapies, Roentgenring 11, 97070 Wuerzburg, Germany

24 E-Mail: oliver.pullig@isc.fraunhofer.de

25 Franziska Ehlicke ($corresponding author)

26 • University Hospital Wuerzburg, Department Tissue Engineering and Regenerative Medicine,

27 Roentgenring 11, 97070 Wuerzburg, Germany

28 E-Mail: franziska.ehlicke@uni-wuerzburg.de

29 Phone: +49 931 3181900

30

31 # Abstract

32 Objective

33 High failure rates of (trauma induced) knee injuries highlight the need to improve current treatment

34 strategies aiming to decrease the number of secondary osteoarthritis developed by patients in later stage

35 [1-3]. In this controlled laboratory study the stimulative effect of mesenchymal stromal cells (MSC) on

36 chondrocyte (CHON) extracellular matrix production was investigated in an *ex vivo* cartilage defect model

37 (chondral vs. full thickness defects) cultured under normoxic (20 % O_2) and physioxic (2 % O_2) conditions.

38 Design

39 Porcine CHON or co-culture of 20 % CHON and 80 % MSC (MIX) were embedded in collagen type I hydrogel,

40 implanted into 4 mm diameter cartilage defects of osteochondral explants and cultured with tissue specific

41 media without addition of TGF-β under normoxia and physioxia. Chondral defects were induced

42 automatically, while full thickness defects were created with biopsy punch. After 28 days of culture,

43 samples were histologically processed, and treatments outcome was evaluated using international

44 cartilage repair society (ICRS)-II scoring.

45 Results

46 Under physioxic conditions, cartilage repair scoring results of the MIX treatment (chondral 8.67 ± 2.42, full

47 thickness 5.67 ± 1.21) were close to those of CHON treatment (chondral 8.17 ± 0.75, full thickness

7.33 ± 1.21). Overall, scoring results were higher in physioxia compared to normoxia conditions in chondral defects, but less or no prevalent for full thickness defects.

Conclusion

Co-culture of CHON with MSC represents a promising approach to stimulate chondrogenic repair and tissue formation in our *ex vivo* model and reduces total amount of CHON needed for cell-based treatment.

Keywords

cartilage defect, *ex vivo* model, cartilage test system, chondrocytes, MSC, collagen type I hydrogel

1 Introduction

Defects of the articulating surface are frequently occuring diseases in the field of orthopedics, traumatology and sports medicine [4]. Around 14 % of patients who suffered from a trauma induced knee injury during their middle ages, including fractures of the tibia, fibula, femur, or patella, develop osteoarthritis in the same knee joint at later age (>65 years) [3]. High risk of failure of more than 20 % in cartilage defect repair require to rethink and improve current cartilage treatment concepts with the aim for long-term repair of cartilage defects [1, 2].

Due to the avascular and aneural character of adult articular cartilage, large defects do not heal spontaneously [5]. Defects that are classified according to International Cartilage Repair Society (ICRS) grade III (defect depth >50 % cartilage depth) and IV (defect reaches subchondral bone) need surgical intervention to repair [6]. Gold standard for defects larger than 2-3 cm^2 is the autologous chondrocyte implantation (ACI), resulting in similar outcome as microfracture [7, 8]. In a recent data analysis for cartilage defects, matrix-associated chondrocyte implantation (M-ACI) showed a significant lower reoperation rate than microfracture 2 years post-op [9]. M-ACI as well as ACI require two surgical

interventions; the first to take a cartilage tissue sample for subsequent chondrocyte isolation and the second one for injection of isolated *in vitro* expanded autologous chondrocytes into defect site.

However, (M-)ACI has two main limitations: Due to the limited number of healthy and non-degenerated chondrocytes, cells have to be expanded *in vitro* to achieve sufficient number of cells needed for the implantation (ACI: 1 Mio/cm², M-ACI: 20 Mio/cm³) [10-12]. Further, chondrocyte-based cartilage treatments, as well as microfracture techniques, result in formation of fibrocartilage, characterized by its inferior mechanical properties and thus lacking functional restoration compared to healthy hyaline cartilage [2, 13-17]. One approach to overcome the limitation of cell number for (M-)ACI treatment are MSC-chondrocyte co-cultures, *e.g.*, 80 % MSC and 20 % chondrocytes, that reduces autologous chondrocyte cell number at same total cell density. Co-cultures of MSCs and chondrocytes have shown to increase cartilaginous matrix production and reduce hypertrophy, associated with MSCs during chondrogenic differentiation [18, 19].

To bring cartilage treatments to the next level, cartilage repair needs to be studied and understood in more detail, starting with basic research questions in a physiologically relevant environment.

An *ex vivo* cartilage defect test system based on osteochondral explants was established by Schwab *et al.*. This test system represents a valuable *ex vivo* platform for biomaterial evaluation in critical size trauma-induced cartilage defects in terms of biocompatibility, biomaterial tissue integration and cartilage repair with higher throughput compared to *in vivo* models. Separated media compartments of the culture device allow for controlled, tissue- and cell-specific nutrient supply during *ex vivo* culture of osteochondral explants [20]. This model also allows direct comparison of different treatment approaches under controlled conditions and has been shown to stimulate cartilage-like tissue formation of chondrocytes or MSCs in osteochondral lesions [21, 22].

However, this defect model was limited to full thickness defects created with a biopsy punch. To date, the creation of defects that do not fully penetrate the cartilage with the help of a biopsy punch or scalpel suffer from low reproducibility and are dependent on the operator. Therefore, an automated device with

97 control over drilling depth to create defects with high reproducibility can overcome this limitation to study
98 chondral wound healing. Of note, the drilling should not harm surrounding cartilage tissue and cell
99 viability, neither by mechanical tissue disruption nor by friction induced heating. For the creation of
100 defects in hard tissues like cartilage or even bone, there is no device available for automated defect
101 creation that meets the above-mentioned requirements.

102 Following, in the present study the defect creation of the *ex vivo* defect model introduced by Schwab *et*
103 *al*. was modified by implementation of a semi-automated drilling device, originally developed to
104 mechanically induce standardized and reproducible wounds in full thickness skin equivalents [23]. Key
105 features of this artificial tissue cutter (ARTcut®) are the sensor controlled optical barrier in combination
106 with a moveable milling machine along x-, y- and z-axis. The light-barrier controlled drilling allows for
107 creation of defects with defined depths in a reproducible set-up. Creation of tissue defects with ARTcut®
108 can be performed under sterile conditions for subsequent *in vitro* or *ex vivo* culture with the possibility to
109 adjust defect geometry and control of defect creation process.

110 Another fact that has been neglected in the studies by Schwab *et al.* is the low oxygen tension present in
111 the articular capsule [24]. It has been shown in literature that low oxygen tension is an important stimulus
112 in chondrogenesis and increases the chondrogenic potential of articular cartilage progenitor cells and
113 MSCs [24-26].

114 Taken together, the present study aimed to investigate two cartilage treatment strategies and the
115 influence of defect depth (full thickness defects and chondral defects) on tissue repair. Additionally, the
116 effect of oxygen tension (normoxia 20 % vs. physioxia 2 %) was studied in both defect and treatment
117 approaches. For the treatment strategies either chondrocytes only (CHON) or a mixture of 80 % MSC and
118 20 % CHON (MIX) were embedded in a collagen type I hydrogel for implantation into cartilage defects in
119 the *ex vivo* osteochondral model without further supplementation of growth factors to elusively study the
120 effect of the culture conditions on cartilage repair.

121 # 2 Methods

122 ## 2.1 Osteochondral cylinders: Isolation, defect creation and *ex vivo* culture

123 Osteochondral cylinders (diameter: 8 mm, height: 5 mm) were isolated from medial femoral condyles of
124 6-8-month-old domestic pigs as previously described [20]. Creation of defects in osteochondral cylinders
125 was carried out either manually or automatically, depending on the intended defect depth: Full thickness
126 defects were manually created with a biopsy punch (diameter 4 mm; Kai Medical, BPP-40F). Chondral
127 defects of 1 mm depth were created using custom-built ARTcut® (Figure 1A), a software-controlled device
128 for automatic wound placement in tissues developed by Fraunhofer ISC and IGB, Wuerzburg [23].
129 Osteochondral cylinders were fixed in support plate (Figure 1C) at specific x- and y-positions, and onset of
130 drilling 1 mm chondral defects (z-axis) was determined with light beam (Figure 1B). For more details on
131 the standardized defect creation process using ARTcut®, see supplementary information.
132 After creation of full thickness or 1 mm chondral defects, the cartilage defects were filled with cell
133 embedded collagen type I hydrogels (**Error! Reference source not found.** 2). For subsequent *ex vivo*
134 culture, osteochondral explants were transferred into custom-made culture platform [20] and cultured for
135 28 days with tissue specific media (Table 1) changed every 3-4 days. The *ex vivo* culture was carried out in
136 a humidified atmosphere at 37°C and 5 % CO_2 (BBD 6220 CO_2 Incubator, Thermo Scientific™) either under
137 normoxic (20 %) or physioxic (2 %) conditions.

138 ## 2.2 Chondrocyte and mesenchymal stromal cells (MSC): isolation and *in vitro* expansion

139 Porcine chondrocytes were isolated from lateral condyles of 6-8 month-old domestic pigs by enzymatic
140 digestion as previously described [20]. Chondrocytes were used at passage 0 – directly after isolation - for
141 embedding in collagen type I hydrogel.
142 Porcine MSC were isolated from bone marrow aspirate (iliac crest) under the approval (reference number:
143 55.2 2532-2-256) of the District Government of Lower Franconia and the local animal welfare committee
144 and performed according to the German Animal Welfare Act and the EU Directive 2010/63/EU. Following

145 gradient centrifugation using Ficoll-Paque (GE Healthcare Bio-Sciences, 17-5442-03), mononuclear cell
146 fraction was expanded in DMEM HG medium (GlutaMax, Gibco 61965) supplemented with 1 ng/mL FGF-
147 2 (R&D Systems, 233-FB-025), 10 % FCS (Gibco, 10270106) and 1 % Antibiotic-Antimycotic (10 U/mL
148 penicillin, 10 µg/mL Streptomycin, 0.25 µg/mL Amphotericin, Gibco, 15240) in humidified atmosphere
149 (37°C, 5 % CO_2). Media change was performed every 3-4 days. MSC were used at passage 2-3 for
150 embedding in collagen type I hydrogel.

151 2.3 Collagen type I hydrogel: hydrogel preparation and cell embedding

152 Cartilage defects were treated with collagen type I hydrogel. Collagen was isolated from rat tails (Wistar
153 IGS Rat; Charles River Laboratories), dissolved in 0.1 % (v/v) acetic acid to a concentration of 4.5 mg/mL,
154 and mixed with half volume of gel neutralizing solution (GNS) to achieve a final concentration of 3 mg/mL.
155 GNS consists of 2x DMEM high glucose (DMEM, PAA Laboratories, G0001,3010), 0.09 M HEPES (Sigma,
156 H3375), 3 % FCS (Bio&Sell, FCS.ADD.0500), 0.05 mg/mL chondroitin sulphate (Sigma, C4384) with pH value
157 adjusted to pH 8.5. Cell embedding was realized by mixing the porcine chondrocytes and/or MSCs in GNS,
158 resulting in a final total cell concentration of 20 Mio/mL hydrogel. Gelation was performed via incubation
159 of GNS collagen solution mixture for 20 min at 37°C under humidified atmosphere.
160 For implantation, two different cell laden constructs, as illustrated in Figure 2, were prepared and each
161 cultured under normoxic and physioxic conditions. 1) CHON were prepared by embedding of chondrocytes
162 in collagen type I hydrogel without expansion at a final density of 20 Mio/mL hydrogel volume; 2) MIX
163 were prepared by mixing 80 % MSC with 20 % chondrocytes at same cell density. CHON and MIX implants
164 were filled into the cartilage defect for gelation at 37°C.

165 ## 2.4 Live-dead viability staining

166 To visualize a possible effect of defect creation process on cell viability of tissue samples, live-dead viability
167 staining was performed (live-dead staining kit for mammalian cells, L3224, Invitrogen). Osteochondral
168 explants were incubated with 4 µM Calcein AM and 2 µM ethidium homodimer-1 in DMEM HG and
169 visualized with fluorescence microscope (494 nm/517 nm and 517 nm/617 nm wavelength) Keyence BZ-
170 9000 (Biorevo). Living cells are stained by Calcein AM in green, dead cells are stained by ethidium
171 homodimer-1 in red.

172 ## 2.5 Histological evaluation

173 Osteochondral explants, harvested on day 0 and day 28, were washed with phosphate buffered saline,
174 fixed for 24 h with 4 % formalin (Roti Histofix, Carl Roth P087.3) and processed with plastic embedding
175 (Technovit T9100, Heraeus Kulzer, 66006735) as detailed described in the supplementary.
176 For immune-histological stainings, antigens were enzymatically retrieved depending on antibody (Table 2).
177 Before incubation with primary antibody over night at 4°C, slides were blocked with 3 % (v/v) H_2O_2 (Carl
178 Roth, 8070) and incubated with 5 % (w/v) bovine serum albumin. All stainings were visualized with
179 Horseradish-peroxidase kit (DCS Innovative, Dako, K3468) following manufacturer`s instructions. Cell
180 nuclei were counterstained with Mayer's hematoxylin (Morphisto, 11895), rehydrated and mounted with
181 Entellan (Merck, 1079610500). All washing steps between blocking or chemical incubation were
182 performed with PBS supplemented with 0.5 % Tween-20 (VWR, 8.22184).

183 ## 2.6 Histological scoring

184 Histological scoring for the evaluation of the immunohistological stainings was performed according to the
185 standardized guidelines of the international cartilage repair society (ICRS-II-Score). All stainings for
186 collagens type I, II, X and aggrecan of this study (n = 2 biological replicates) were evaluated blinded by
187 three independent operators according to the criteria summarized in Table 3. Maximum possible score for
188 the here reported study was 12 points.

189 ## 2.7 Statistics

190 Statistical analysis was performed with GraphPad Prism 6.07. Scoring values obtained from two
191 independent experiments, each evaluated by three examinators were used for statistical analysis,
192 resulting in $n = 6$ for each experimental group (Figure 2). Following tests for outlier and Gaussian
193 distribution, the data was either compared using an unpaired t-test (normally distributed values) or a
194 Mann-Whitney test (not normally distributed values). A p-value <0.05 was considered statistically
195 significant.

196 # 3 Results

197 ## 3.1 Chondral defect creation with ARTcut®

198 ARTcut® (Figure 1) represents an automated device for reproducible creation of chondral defects (1 mm
199 in depth; Figure 3A). Main advantage of using the ARTcut® is the ability to create defined chondral defects
200 with a flat bottom to allow a tide and uniform contact with any solid pre-formed cylindrical implant, for
201 example bioprinted constructs with flat bottom.

202 The laser beam to detect the surface of every single osteochondral explant is the unique feature of the
203 ARTcut® to define the onset of the drilling, thus all defects result with the same depth. Chondral cartilage
204 defect induced with ARTcut® appeared as a well-defined rectangular defect boundary in cross section
205 (diameter: 4 mm, height: 1 mm) with flat bottom (Figure 3B). In contrast, the manually created defect
206 (using biopsy punch) resulted in a half-round shape and required removing of residual cartilage tissue with
207 a second tool (*e.g.,* a sharp spoon) shown in Figure 3C. Following, the accuracy of chondral defect
208 geometry was much lower in manual procedure - using biopsy punch - compared to software – using
209 automated ARTcut®.

210 The automated defect creation took less than 5 sec and thus heating of tissue due to friction and rotation
211 during drilling was very unlikely. Microscopic images of live-dead stainings of osteochondral explants with

212 1 mm cartilage defects (diameter: 4 mm) confirmed no indications of cell death after tissue defect
213 creation, neither with ARTcut® nor with biopsy punch (Figure 3D-E).
214 For the creation of full thickness cartilage defects, the ARTcut® was not required, since the bottom of the
215 defect was given by the cartilage-bone interface. This two-tissue interface was easily separated using
216 biopsy punch by pulling out the upper cartilage part.

217 3.2 Evaluation of cartilage treatments in the *ex vivo* model

218 The results of our study demonstrate the feasibility and reproducibility of the *ex vivo* cartilage test system
219 as a platform to compare cartilage repair strategies: Scoring results of the co-culture (MIX) are close to the
220 CHON treatment in chondral and full thickness defects. Results of the adapted ICRS-II scoring are shown
221 in Figure 4.
222 Under physioxic conditions, scoring results of defect repair after co-culture treatment (MIX) was
223 significantly higher ($p = 0.0218$) in chondral defect than in full thickness defects. Scoring values of CHON
224 treatment in chondral and full thickness experimental groups did not differ much (n.s. $p = 0.1828$). At
225 physioxic conditions the scoring value was significant higher for CHON treatment compared to MIX
226 treatment in full thickness defects ($p = 0.0384$).
227 Under normoxic conditions, full thickness defects reached higher scoring values compared to the chondral
228 defects.
229 Comparing the outcome of same defect depth and treatment group (cell type), but cultured under
230 physioxic or normoxic conditions, the oxygen tension plays only a significant role in chondral defects using
231 MIX ($p = 0.0451$, higher scoring values under physioxic conditions) and in full thickness defects treated
232 with CHON ($p = 0.0316$, lower scoring values under physioxic conditions).
233 Overall, treatment of the two defect depths with MIX showed slightly reduced scoring values compared
234 to the CHON treatment group. Only exception is MIX chondral (physioxia) with a slightly higher value as

235 the corresponding one for CHON. The results of the MIX treatment groups also tend to spread more than
236 the CHON treatment group independently of defect depth and oxygen tension.

237 4 Discussion

238 The choice of optimal treatment approach for cartilage repair is dependent on the size and depth of the
239 cartilage defect and thus the severity of pathological condition.
240 To mimic these different pathological defect scenarios, the implementation of the ARTcut® allowed to
241 overcome the low reproducibility of manual induced chondral defects. So far, there is no other automated
242 defect creation device published that has comparable features, namely possibility to select different
243 drilling parameters within one run and the application of one device for a wide range of soft and hard
244 tissues or tissue equivalents, as it is demonstrated with the ARTcut®. The induction of defects in
245 osteochondral explants allows to compare different cell-based treatment approaches by implantation of
246 cell loaded materials into the defects or to study the effect of defect depth on repair in an *ex vivo* model.
247 The software-controlled drilling parameters allow for standardized and reproducible defect creation in
248 other soft and hard tissues including bone tissue as well. *In vitro* as well as *ex vivo* studies require sample
249 procession at high throughput rates under a negative microbial environment. ARTcut® device addresses
250 these demands, resulting in higher methodological accuracy and reproducibility, compared to manual
251 procedure using biopsy punch.
252 Current treatments of small or large cartilage defects mainly aim on pain and symptom relief rather than
253 on functional tissue repair [27]. From a scientific point of view, there is way for improvement of cartilage
254 defects, especially on long term results. Material-assisted as well as cell-based therapies, including (M-)
255 ACI, AMIC and microfracture, tend to result in formation of mechanical inferior fibrocartilage in long term
256 follow up [27-29]. Moreover, the treatment of large defects with autologous cells are limited due to the
257 high number of chondrocytes needed for the current techniques. Therefore, in this laboratory-controlled
258 study, an *ex vivo* osteochondral defect model was modified to screen cell-based approaches to treat

259 chondral and full thickness cartilage defects. Different cell types, namely chondrocytes and MSCs, were
260 embedded in collagen type I hydrogel (CHON or MIX) and implanted in trauma induced chondral and full
261 thickness defects. A stimulative and beneficial effect of MIX treatment (20 % CHON and 80 % MSCs) was
262 observed regarding cartilaginous matrix formation with the main advantage to reduce the overall number
263 of CHON used for traditional ACI treatment.

264 Promising results regarding cartilage matrix production were obtained comparing CHON and MIX in
265 chondral and full thickness defects in the *ex vivo* model. The MIX treatment reduces the amount of
266 autologous cartilage tissue needed for chondrocyte isolation, since chondrocytes represented only 20 %
267 of the total cell number in our model. Several *in vitro* studies and *in silico* models have shown that
268 chondrocytes in co-culture with MSCs increase the chondrogenic differentiation potential [18, 19, 30, 31].
269 Scalzone *et al.* reported of an enhanced chondrocyte activity measured by proteoglycan and collagen type
270 II production after co-culture with MSC compared to chondrocyte monoculture both embedded in
271 chitosan based hydrogels [19].

272 One advantage of the co-culture approach – when clinically applied – would be the one-step procedure,
273 addressing the surgical intervention of the knee joint, for the treatment of the cartilage defect: The
274 reduced number of chondrocytes in the MIX treatment can be isolated intra-operatively without
275 expansion and thus reduced the risk of chondrocyte dedifferentiation [32]. Further, the required MSCs,
276 *e.g.,* can be harvested independently form the knee surgery from bone marrow aspirate in a minimal
277 invasive procedure with subsequent expansion prior to the cartilage repair procedure to ensure a
278 sufficient number of MSCs.

279 Considering the absence of TGF-β in the culture media, which is known to drive MSC chondrogenesis [33],
280 the here reported cartilage repair solely derives from the stimulating effect of the surrounding
281 osteochondral tissue, cell-cell signaling of the cell laden implants and the culture conditions.

282 Results of a similar *ex vivo* model, based on horse and bovine osteochondral explants, suggested that the
283 presence of the osteochondral tissue in the explants increase cartilage-like matrix deposition compared to
284 free swelling conditions of cell seeded material only [21, 22].
285 Beside the cell source, the influence of oxygen tension (normoxia 20 % O_2, physioxia 2 % O_2) was studied
286 during the *ex vivo* culture on chondrogenic matrix deposition, resulting in different outcomes between the
287 treatment groups in chondral and full thickness defects. Based on the histological scoring, our results
288 showed that the oxygen tension only plays a role in chondral defects - marked by elevated matrix
289 production. In contrast, full thickness defects showed different response in cartilage-like matrix deposition
290 related to the treatment approach: While higher scoring values were reached with CHON treatment under
291 normoxic conditions, the pMIX treatment did not show differences comparing physioxic and normoxic
292 conditions. Physioxic conditions resulted in an increase in cartilaginous matrix deposition in chondral
293 defects compared to full thickness defects independently of the used cell type (CHON, MIX). Once the
294 defect reaches the cartilage-bone interface, the cells in the implant receive stimuli from the subchondral
295 bone that seem to counteract with the physioxic induced stimuli in the here presented model. One
296 explanation of the differential cell response to oxygen tension in chondral and full thickness defects may
297 originate from the variation in oxygen tension present in the human body. Chondrocytes are exposed to
298 lower oxygen tension in avascular cartilage (2-5 %) [34], synovial fluid and the synovial capsule (6.5-9.0 %)
299 [25, 35], with an increasing oxygen level in the bone marrow of subchondral bone (>7 %) [26, 36] and a
300 maximum of 12 % in arterial blood [37]. Once the cartilage defect progresses to the exposure of the
301 subchondral bone in patients, chondrocytes within the defect are exposed to higher levels of oxygen
302 present in the bone supplied by vascular invasion [38]. It has been shown that low oxygen inhibits the
303 degradation of hypoxia induced factors (HIF) [39]. HIFs are described to be essential for maintaining CHON
304 homeostasis and extracellular matrix synthesis and activate the transcription of genes [40].
305 While the here presented results are consistent, traceable and in line with literature, there is one limitation
306 in the current experimental setup: Due to limitations in availability of human healthy osteochondral tissue

307 – absence of any osteoarthritic phenotype – the authors decided to use porcine tissue instead, as
308 introduced by Schwab *et al.* [20]. The performance of an extensive comparative *ex vivo* study comprising
309 three parameters – namely 1) defect depth (chondral vs. full thickness), 2) different cell types for defect
310 filling and treatment (100 % chondrocytes vs. 20 % chondrocytes and 80 % MSCs), and 3) oxygen tension
311 (physioxia vs. normoxia) requires tissue material in the required quantity and of similar quality. Due to the
312 well-known donor issues associated with donor variability of human tissue and the already mentioned
313 limited availability of healthy human osteochondral tissue, this could not be achieved for human tissue
314 [41, 42]. In contrast, the use of porcine tissue isolated from one pig population (similar age; grown up
315 under equal conditions) minimizes the donor variation and represents a tissue source for healthy and non-
316 degenerated tissues with higher reproducibility.
317 Overall, the results obtained in this study strongly indicate that the surrounding tissue of the
318 osteochondral explants plays a crucial role in the defect repair, addressing chondral or full thickness
319 defects, and that the oxygen tension additionally stimulates the outcome in a defect depth dependent
320 way. However, the exact mechanism controlling success or failure of a treatment approach are not fully
321 understood and require further research. Despite the advantage of the here reported model, the mimicry
322 of the complex 3D environment present in the knee joint with the additional ability to reproducibly create
323 (trauma induced) defects, this model has its potential in pre-screening several biomaterials or treatment
324 approaches, but best candidates still require further pre-clinical and clinical testing to confirm obtained
325 results.
326 To conclude, in this *ex vivo* study two cell-based approaches (CHON vs. MIX embedded in collagen type I
327 hydrogel) for the treatment of chondral and full thickness defects, cultured under normoxic and physioxic
328 conditions, were compared on their cartilage repair potential. Independently of defect depth, the co-
329 culture of chondrocytes and MSC (MIX) has proven scoring results close to those of CHON treatment.
330 Hence, usage of MIX could be a promising approach to reduce the number of chondrocytes to one fifth
331 and thus the amount of tissue for harvest and accompanied side morbidities for the patient. Further, in

332 this experimental set up the oxygen tension showed an influence in a defect depth dependent way: an
333 increased extracellular matrix production resulted in chondral defect under physioxic conditions but was
334 not present in full thickness defects. This finding of defect dependent stimulus of oxygen tension on
335 cartilage repair has not been reported in literature before.

336 Acknowledgements

337 The authors thank Andreas Diegeler (Fraunhofer ISC, Bronnbach) for technical support of the ARTcut®.
338 Thanks also to Sebastian Naczenski for establishing the protocol for wounding of osteochondral explants
339 using ARTcut® device. Finally, we would like to thank Heike Walles for her support.

340

341 Author contribution

342 Conception and design of the study: Franziska Ehlicke and Andrea Schwab; Acquisition of data: Alexa
343 Buss and Andrea Schwab; Analysis and interpretation of data: Andrea Schwab, Alexa Buss, Franziska
344 Ehlicke and Oliver Pullig; Manuscript drafting: Andrea Schwab and Alexa Buss; Revision of the
345 manuscript: Franziska Ehlicke and Oliver Pullig; Final approval: Franziska Ehlicke, Andrea Schwab, Alexa
346 Buss and Oliver Pullig; Funding: Franziska Ehlicke and Alexa Buss.

347 Role of funding Sources

348 This work was financially supported by the European Union Seventh Framework Programme (FP7/2007-
349 2013) under grant agreement no 309962 (HydroZONES). Graduate School of Life Sciences (University of
350 Wuerzburg) is acknowledged for providing medical scholarship.

351 Competing interest statement

352 The authors declare no conflict of interest.

353 Ethics approval and consent to participate

354 Animal experiment was approved (reference number: 55.2 2532-2-256) by the District Government of
355 Lower Franconia and the local animal welfare committee and performed according to the German Animal
356 Welfare Act and the EU Directive 2010/63/EU. Following heparinization of the pig, porcine MSCs were
357 obtained by bone marrow aspiration.

References

[1] A.R. Martín, J.M. Patel, H.M. Zlotnick, J.L. Carey, R.L. Mauck, Emerging therapies for cartilage regeneration in currently excluded 'red knee' populations, npj Regenerative Medicine 4(1) (2019) 12.

[2] J.D. Wylie, M.K. Hartley, A.L. Kapron, S.K. Aoki, T.G. Maak, Failures and Reoperations After Matrix-Assisted Cartilage Repair of the Knee: A Systematic Review, Arthroscopy 32(2) (2016) 386-92.

[3] A.C. Gelber, M.C. Hochberg, L.A. Mead, N.Y. Wang, F.M. Wigley, M.J. Klag, Joint injury in young adults and risk for subsequent knee and hip osteoarthritis, Ann Intern Med 133(5) (2000) 321-8.

[4] W. Widuchowski, J. Widuchowski, T. Trzaska, Articular cartilage defects: study of 25,124 knee arthroscopies, Knee 14(3) (2007) 177-82.

[5] A.J. Sophia Fox, A. Bedi, S.A. Rodeo, The basic science of articular cartilage: structure, composition, and function, Sports Health 1(6) (2009) 461-8.

[6] E.A. Makris, A.H. Gomoll, K.N. Malizos, J.C. Hu, K.A. Athanasiou, Repair and tissue engineering techniques for articular cartilage, Nat Rev Rheumatol 11(1) (2015) 21-34.

[7] B.J. Cole, C. Pascual-Garrido, R.C. Grumet, Surgical management of articular cartilage defects in the knee, J Bone Joint Surg Am 91(7) (2009) 1778-90.

[8] A.K. Dewan, M.A. Gibson, J.H. Elisseeff, M.E. Trice, Evolution of autologous chondrocyte repair and comparison to other cartilage repair techniques, Biomed Res Int 2014 (2014) 272481.

[9] P. Niemeyer, T. Schubert, M. Grebe, A. Hoburg, Matrix-Associated Chondrocyte Implantation Is Associated With Fewer Reoperations Than Microfracture: Results of a Population-Representative, Matched-Pair Claims Data Analysis for Cartilage Defects of the Knee, Orthop J Sports Med 7(10) (2019) 2325967119877847.

[10] M. Brittberg, A. Lindahl, A. Nilsson, C. Ohlsson, O. Isaksson, L. Peterson, Treatment of deep cartilage defects in the knee with autologous chondrocyte transplantation, N Engl J Med 331(14) (1994) 889-95.

[11] M. Mumme, A. Barbero, S. Miot, A. Wixmerten, S. Feliciano, F. Wolf, A.M. Asnaghi, D. Baumhoer, O. Bieri, M. Kretzschmar, G. Pagenstert, M. Haug, D.J. Schaefer, I. Martin, M. Jakob, Nasal chondrocyte-based engineered autologous cartilage tissue for repair of articular cartilage defects: an observational first-in-human trial, Lancet (London, England) 388(10055) (2016) 1985-1994.

[12] R.L. Davies, N.J. Kuiper, Regenerative Medicine: A Review of the Evolution of Autologous Chondrocyte Implantation (ACI) Therapy, Bioengineering (Basel) 6(1) (2019).

[13] J.D. Lamplot, K.A. Schafer, M.J. Matava, Treatment of Failed Articular Cartilage Reconstructive Procedures of the Knee: A Systematic Review, Orthop J Sports Med 6(3) (2018) 2325967118761871.

[14] G. Merkely, T. Ogura, J. Ackermann, A. Barbieri Mestriner, A.H. Gomoll, Clinical Outcomes after Revision of Autologous Chondrocyte Implantation to Osteochondral Allograft Transplantation for Large Chondral Defects: A Comparative Matched-Group Analysis, Cartilage (2019) 1947603519833136.

399 [15] K. Mithoefer, T. McAdams, R.J. Williams, P.C. Kreuz, B.R. Mandelbaum, Clinical efficacy of
400 the microfracture technique for articular cartilage repair in the knee: an evidence-based
401 systematic analysis, Am J Sports Med 37(10) (2009) 2053-63.
402 [16] P.C. Kreuz, M.R. Steinwachs, C. Erggelet, S.J. Krause, G. Konrad, M. Uhl, N. Sudkamp, Results
403 after microfracture of full-thickness chondral defects in different compartments in the knee,
404 Osteoarthritis Cartilage 14(11) (2006) 1119-25.
405 [17] J.L. Carey, Fibrocartilage Following Microfracture Is Not as Robust as Native Articular
406 Cartilage: Commentary on an article by Aaron J. Krych, MD, et al.: "Activity Levels Are Higher
407 After Osteochondral Autograft Transfer Mosaicplasty Than After Microfracture for Articular
408 Cartilage Defects of the Knee. A Retrospective Comparative Study", JBJS 94(11) (2012).
409 [18] L. Bian, D.Y. Zhai, R.L. Mauck, J.A. Burdick, Coculture of human mesenchymal stem cells and
410 articular chondrocytes reduces hypertrophy and enhances functional properties of engineered
411 cartilage, Tissue engineering. Part A 17(7-8) (2011) 1137-1145.
412 [19] A. Scalzone, A.M. Ferreira, C. Tonda-Turo, G. Ciardelli, K. Dalgarno, P. Gentile, The interplay
413 between chondrocyte spheroids and mesenchymal stem cells boosts cartilage regeneration
414 within a 3D natural-based hydrogel, Sci Rep 9(1) (2019) 14630.
415 [20] A. Schwab, A. Meeuwsen, F. Ehlicke, J. Hansmann, L. Mulder, A. Smits, H. Walles, L. Kock, Ex
416 vivo culture platform for assessment of cartilage repair treatment strategies, ALTEX 34(2) (2017)
417 267-277.
418 [21] V.H.M. Mouser, N.M.M. Dautzenberg, R. Levato, M.H.P. van Rijen, W.J.A. Dhert, J. Malda, D.
419 Gawlitta, Ex vivo model unravelling cell distribution effect in hydrogels for cartilage repair,
420 ALTEX 35(1) (2018) 65-76.
421 [22] M.L. de Vries-van Melle, R. Narcisi, N. Kops, W.J. Koevoet, P.K. Bos, J.M. Murphy, J.A.
422 Verhaar, P.M. van der Kraan, G.J. van Osch, Chondrogenesis of mesenchymal stem cells in an
423 osteochondral environment is mediated by the subchondral bone, Tissue Eng Part A 20(1-2)
424 (2014) 23-33.
425 [23] A. Rossi, A. Appelt-Menzel, S. Kurdyn, H. Walles, F. Groeber, Generation of a three-
426 dimensional full thickness skin equivalent and automated wounding, J Vis Exp (96) (2015).
427 [24] G. Pattappa, R. Schewior, I. Hofmeister, J. Seja, J. Zellner, B. Johnstone, D. Docheva, P.
428 Angele, Physioxia Has a Beneficial Effect on Cartilage Matrix Production in Interleukin-1 Beta-
429 Inhibited Mesenchymal Stem Cell Chondrogenesis, Cells 8(8) (2019).
430 [25] G. Pattappa, B. Johnstone, J. Zellner, D. Docheva, P. Angele, The Importance of Physioxia in
431 Mesenchymal Stem Cell Chondrogenesis and the Mechanisms Controlling Its Response, Int J Mol
432 Sci 20(3) (2019).
433 [26] D.E. Anderson, B.D. Markway, D. Bond, H.E. McCarthy, B. Johnstone, Responses to altered
434 oxygen tension are distinct between human stem cells of high and low chondrogenic capacity,
435 Stem Cell Res Ther 7(1) (2016) 154.
436 [27] U. Horas, D. Pelinkovic, G. Herr, T. Aigner, R. Schnettler, Autologous chondrocyte
437 implantation and osteochondral cylinder transplantation in cartilage repair of the knee joint. A
438 prospective, comparative trial, J Bone Joint Surg Am 85(2) (2003) 185-92.
439 [28] J.R. Steadman, K.K. Briggs, J.J. Rodrigo, M.S. Kocher, T.J. Gill, W.G. Rodkey, Outcomes of
440 microfracture for traumatic chondral defects of the knee: average 11-year follow-up,
441 Arthroscopy 19(5) (2003) 477-84.

[29] J.L. Carey, Fibrocartilage following microfracture is not as robust as native articular cartilage: commentary on an article by Aaron J. Krych, MD, et al.: "Activity levels are higher after osteochondral autograft transfer mosaicplasty than after microfracture for articular cartilage defects of the knee. A retrospective comparative study", J Bone Joint Surg Am 94(11) (2012) e80.
[30] M.J. Chen, J.P. Whiteley, C.P. Please, A. Schwab, F. Ehlicke, S.L. Waters, H.M. Byrne, Inducing chondrogenesis in MSC/chondrocyte co-cultures using exogenous TGF-β: a mathematical model, Journal of Theoretical Biology 439 (2018) 1-13.
[31] T.W. Kim, M.C. Lee, H.C. Bae, H.-S. Han, Direct Coculture of Human Chondrocytes and Synovium-Derived Stem Cells Enhances In Vitro Chondrogenesis, Cell J 20(1) (2018) 53-60.
[32] K. von der Mark, V. Gauss, H. von der Mark, P. Muller, Relationship between cell shape and type of collagen synthesised as chondrocytes lose their cartilage phenotype in culture, Nature 267(5611) (1977) 531-2.
[33] B. Johnstone, T.M. Hering, A.I. Caplan, V.M. Goldberg, J.U. Yoo, In vitro chondrogenesis of bone marrow-derived mesenchymal progenitor cells, Exp Cell Res 238(1) (1998) 265-72.
[34] S. Zhou, Z. Cui, J.P.G. Urban, Factors influencing the oxygen concentration gradient from the synovial surface of articular cartilage to the cartilage–bone interface: A modeling study, Arthritis & Rheumatism 50(12) (2004) 3915-3924.
[35] K. Lund-Olesen, Oxygen tension in synovial fluids, Arthritis Rheum 13(6) (1970) 769-76.
[36] A. Carreau, B. El Hafny-Rahbi, A. Matejuk, C. Grillon, C. Kieda, Why is the partial oxygen pressure of human tissues a crucial parameter? Small molecules and hypoxia, J Cell Mol Med 15(6) (2011) 1239-53.
[37] M. Marenzana, T.R. Arnett, The Key Role of the Blood Supply to Bone, Bone Research 1(1) (2013) 203-215.
[38] J. Filipowska, K.A. Tomaszewski, L. Niedzwiedzki, J.A. Walocha, T. Niedzwiedzki, The role of vasculature in bone development, regeneration and proper systemic functioning, Angiogenesis 20(3) (2017) 291-302.
[39] A. Kremer, M. Wussmann, M. Herrmann, M. Raghunath, H. Walles, Ciclopirox olamine promotes the angiogenic response of endothelial cells and mesenchymal stem cells, Clin Hemorheol Microcirc 73(2) (2019) 317-328.
[40] J. Fernandez-Torres, Y. Zamudio-Cuevas, G.A. Martinez-Nava, A.G. Lopez-Reyes, Hypoxia-Inducible Factors (HIFs) in the articular cartilage: a systematic review, Eur Rev Med Pharmacol Sci 21(12) (2017) 2800-2810.
[41] H.X. Chang, L. Yang, Z. Li, G. Chen, G. Dai, Age-related biological characterization of mesenchymal progenitor cells in human articular cartilage, Orthopedics 34(8) (2011) e382-8.
[42] M. Kim, I.E. Erickson, A.H. Huang, S.T. Garrity, R.L. Mauck, D.R. Steinberg, Donor Variation and Optimization of Human Mesenchymal Stem Cell Chondrogenesis in Hyaluronic Acid, Tissue Eng Part A 24(21-22) (2018) 1693-1703.
[43] A. Schwab, Development of an osteochondral cartilage defect model, Julius-Maximilians University, Wuerzburg 2017.

483 ## Figure Legends

484 Figure 1: Artificial tissue cutter (ARTcut®): A) View of the computerized numerical controlled device
485 equipped with B) optical barrier (white arrow indicates the laser light beam) and a C) supporting plate to
486 fix the samples and place on the bottom of the machine (marked with black star). Reprinted from Schwab
487 2017 [43]

488 Figure 2: Schematic overview of all experimental groups: Full thickness and chondral defects of
489 osteochondral explants were treated with collagen type I hydrogel (grey) either containing chondrocytes
490 (CHON, blue) or MIX (80 % MSC and 20 % chondrocytes), implanted in chondral or full thickness defects
491 and cultured *ex vivo* under normoxic (20 % O_2, blue frame) or physioxic conditions (2 % O_2, red frame).

492 Figure 3: Osteochondral explant cross section with chondral defect. A) Schematic illustration of A) 4 mm
493 chondral defect. B-E) Comparison of chondral defect created automated with ARTcut® (B) and manually
494 with biopsy punch (C) (scale bar 500 µm). D-E) Live-dead staining of explant cross section highlighting
495 accurate borders of defect induced with ARTcut® (D) and more irregular shaped geometry of manually
496 induced defect (E) (scale bar 200 µm). Reprinted from Schwab 2017 [43].

497 Figure 4: Evaluation of defect repair after 28 days *ex vivo* culture. Macroscopic images of full thickness and
498 chondral defects (diameter 4 mm) treated with A) porcine Chondrocytes (CHON) or B) co-culture of
499 porcine MSC and CHON (MIX). Red frame indicates culture under physioxic, blue frame under normoxic
500 oxygen tension. Macroscopically, there are no obvious differences comparing full thickness and chondral
501 defects. C-D) Scoring evaluation of cartilage repair strategies in the *ex vivo* model (mean ± standard
502 deviation with single scoring results as dots resp. listed values for 1st and 2nd biological replicate). Unpaired
503 t-test * $p < 0.05$, ** $p < 0.01$.

Figure 1

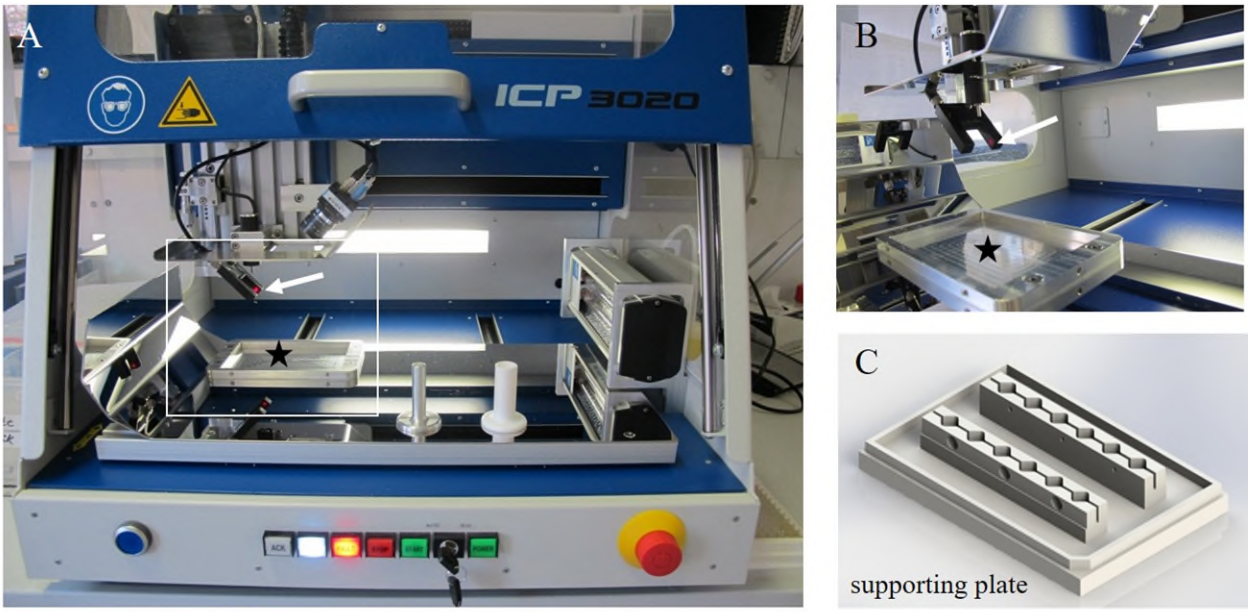

506 Figure 2

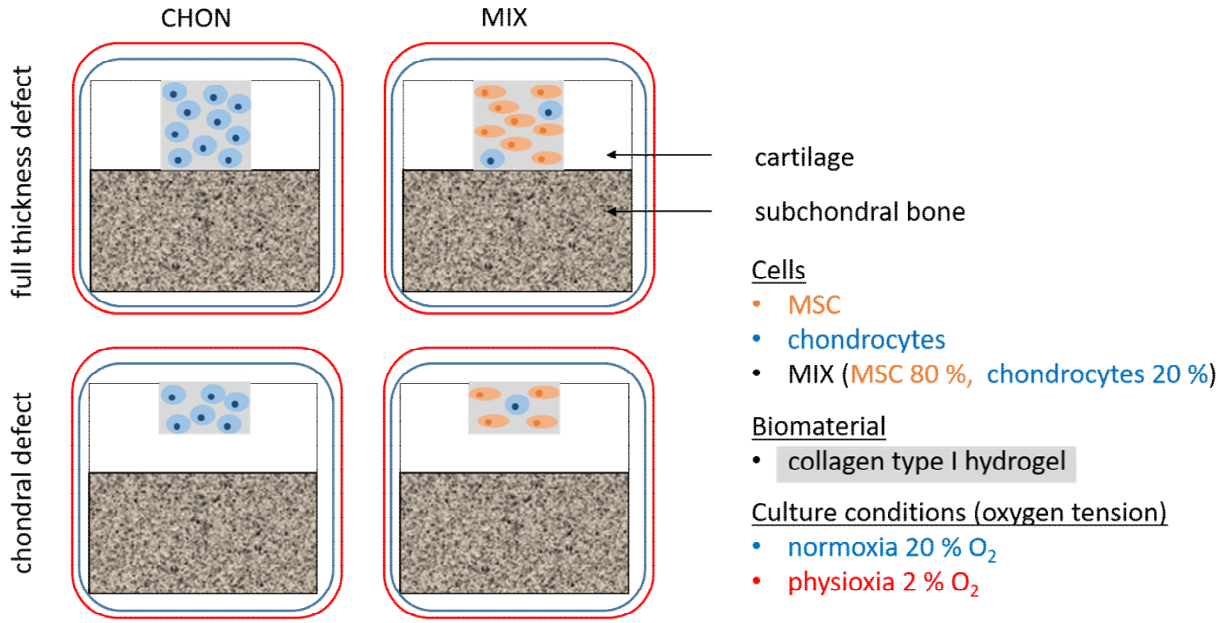

507

508 Figure 3

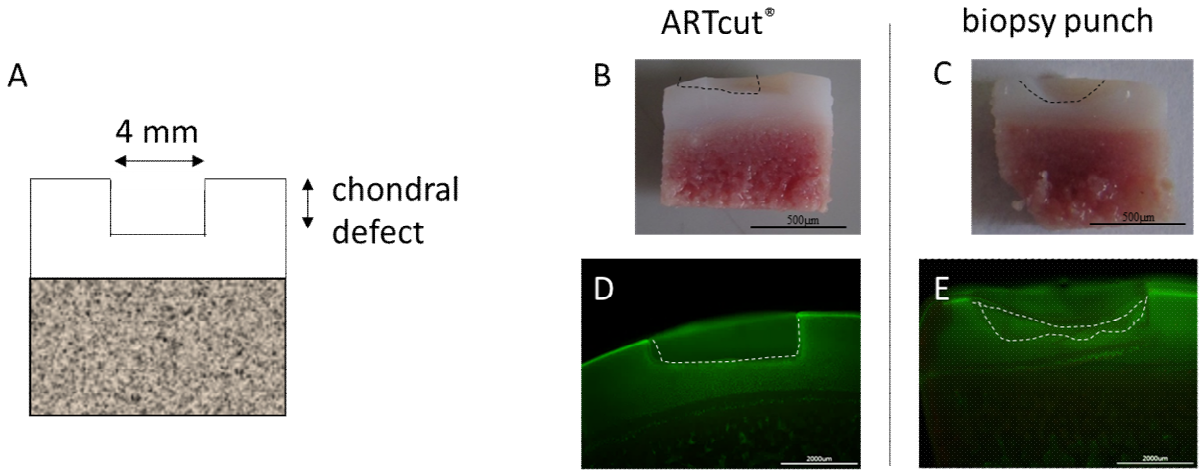

509

510 Figure 4

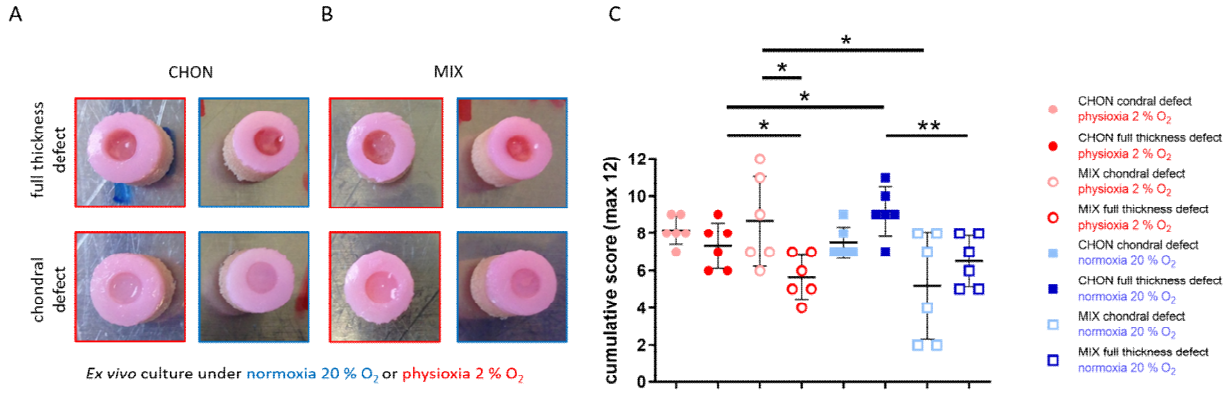

D

		CHON		MIX	
	Cumulative score (max 12)	**Physioxia (2 % O_2)**	**Normoxia (20 % O_2)**	**Physioxia (2 % O_2)**	**Normoxia (20 % O_2)**
full thickness defect	1st biological replicate	9; 8; 8	9; 9; 7	6; 7; 4	8; 8; 7
	2nd biological replicate	7; 6; 6	9; 11; 10	5; 7; 5	5; 5; 6
	Mean ± standard deviation	**7.33 ± 1.21**	**9.17 ± 1.33**	**5.67 ± 1.21**	**6.5 ± 1.38**
chondral defect	1st biological replicate	7; 8; 9	7; 7; 7	11; 9; 12	4; 2; 2
	2nd biological replicate	8; 9; 8	9; 8; 7	7; 7; 6	8; 8; 7
	Mean ± standard deviation	**8.17 ± 0.75**	**7.50 ± 0.84**	**8.67 ± 2.42**	**5.17 ± 2.86**

511

512 Table 1: Composition of bone and cartilage media for *ex vivo* culture of osteochondral explants.

	Cartilage media	Bone media	Supplier
DMEM GlutaMAX (high glucose)	98 %	89 %	Gibco 61965
Antibiotics	10 U/mL penicillin, 10 µg/mL Streptomycin, 0.25 µg/mL Amphotericin (1 % (v/v))	10 U/mL penicillin, 10 µg/mL Streptomycin, 0.25 µg/mL Amphotericin (1 % (v/v))	Gibco, 15240
Sodium-pyruvate	1 mM	-	Gibco, 11360
L-ascorbic acid-2-phosphate	50 µg/mL	50 µg/mL	Wako chemicals, 013-19641
L-proline	40 µg/mL	-	Sigma-Aldrich, P5607
Dexamethasone	100 nM	100 nM	Sigma-Aldrich, D4902
fetal bovine serum (FBS)		10 % (v/v)	Gibco, 10270106
Insulin-transferrin-selenin	1 % (v/v)	-	ITS^{+}-premix, Gibco, Life Technologies, 32430
β-glycerophosphate	-	10 mM	Sigma-Aldrich, G9422

513

514 Table 2: List of antibodies for immune-histological stainings.

Antibody	clone	Dilution and final antibody concentration	Antigen retrieval	Antibody supplier
Collagen type I	EPR7785	1:1000; 0.875 µg/mL	pepsin & hyaluronidase	Abcam, ab138492
Collagen type II	II-4C11	1:1000; 1 µg/mL	pepsin & hyaluronidase	MP Bio, 63171
Collagen type X	COL-10	1:4000; 0.25 µg/mL	pronase	Sigma-Aldrich, C7974
Aggrecan	EPR7785	1:2000; 0.5 µg/mL	pronase	Invitrogen, AHP0012

515

516

517 Table 3: Criteria for evaluating immune histological stainings with modified ICRS-II-Score with maximum of 12 points (0-3 scores

518 for each criteria judging the uniformity and darkness of aggrecan, collagen type I, II and X staining).

ICRS-II-Scoring	**Uniformity and darkness* of Aggrecan stain**
	0: No stain, 1: Weak staining of poorly formed matrix, 2: Moderately even staining ,3: Even dark stain
	Uniformity and darkness* of Collagen type II stain
	0: No stain, 1: Weak staining of poorly formed matrix, 2: Moderately even staining ,3: Even dark stain
	Uniformity and darkness* of Collagen type I stain
	3: No stain, 2: Weak staining of poorly formed matrix, 1: Moderately even staining 0: Even dark stain
	Uniformity and darkness* of Collagen type X stain
	3: No stain, 2: Weak staining of poorly formed matrix, 1: Moderately even staining 0: Even dark stain

519

520